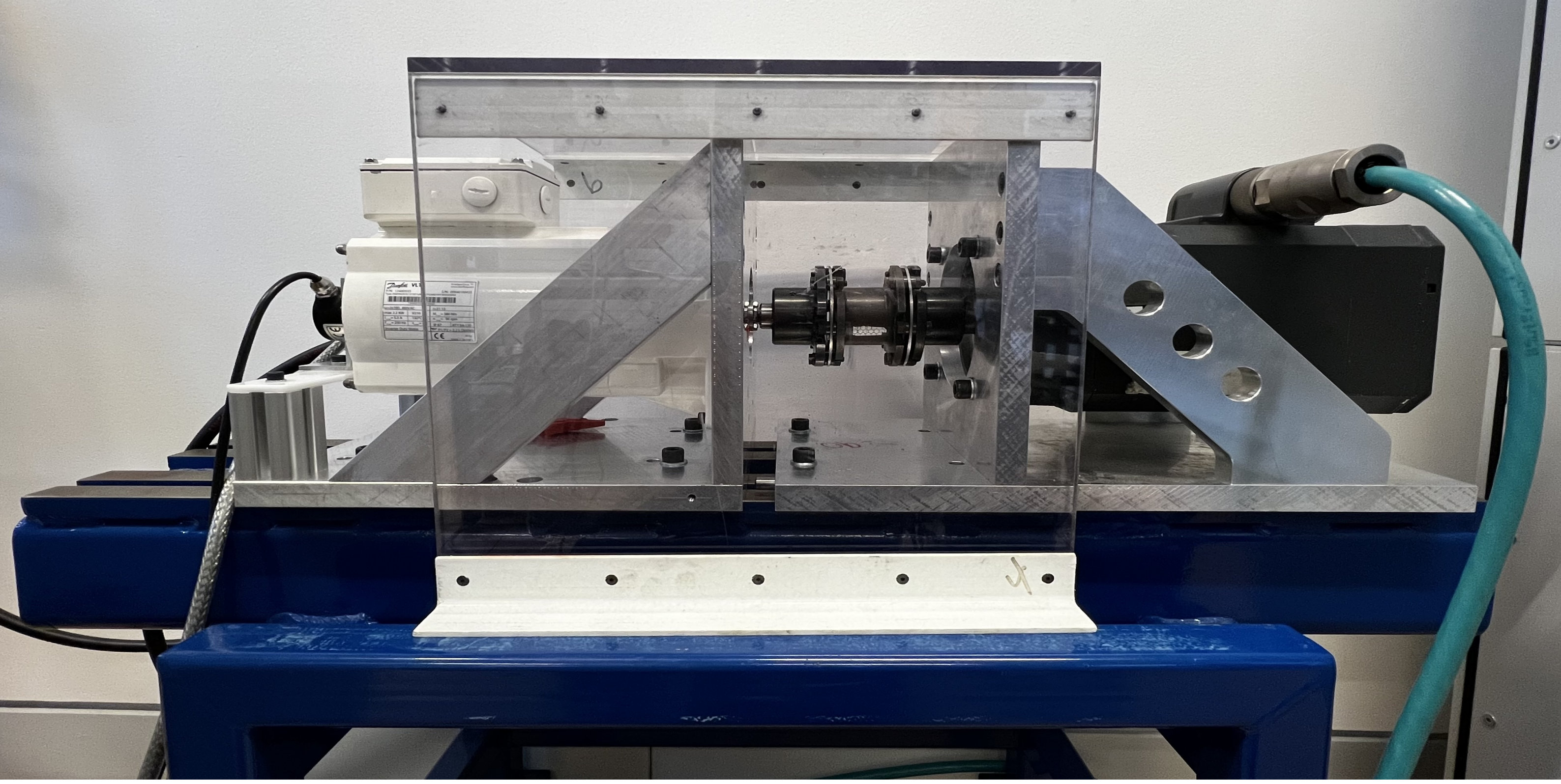

On-line Maximum Torque Per Ampere Tracking Controller For Permanent Magnet Synchronous Machine Drive Systems

Nora Zeitoun

Power Electronics and Drives

Master Thesis

AAU Energy
Aalborg University
http://www.aau.dk

AALBORG UNIVERSITY
STUDENT REPORT

Title:
On-line Maximum Torque Per Ampere Tracking Controller For Permanent Magnet Synchronous Machine Drive Systems

Theme:
Master Thesis

Project Group:
PED4-1047

Participant(s):
Nora Zeitoun

Supervisor(s):
Kaiyuan Lu

Page Numbers: 46

Date of Completion:
March 1, 2024

Abstract:

Maximum Torque Per Ampere (MTPA) control is a common approach to achieve high efficiency in modern electric machine drive systems. This thesis investigates and analyzes on-line MTPA tracking techniques for Surface Mounted Permanent Magnet Synchronous Machine (SPMSM) and for Interior Permanent Magnet Synchronous Machine (IPMSM). The candidate technique is tested on SPMSM and IPMSM platforms. The tracking accuracy, reliability, and responding speed during transients are examined under different operating conditions.

Preface

This thesis is made by Electrical Energy Engineering student from Aalborg University.

Reading Guide

The build-up in this project is chronological. This means that the chapters, sections, and subsections appear as numbered. A table of contents is included, listing the chapters and sections as they appear in the report. Tables, equations, and figures are referred to in the report as a number combination combined of the chapter number and the number of elements in the chapter, for example, equation two in chapter 2 will be referred to as Equation 2.2. A short caption below the figures and tables describing the content will be present. A nomenclature is made, where all indexes used in the report are presented with a short description and the corresponding SI unit. Also, acronyms used in the report are presented in the nomenclature.

Nomenclature

Special Symbols and Denotations

Symbol	Description	Unit
f	Frequency	[Hz]
I	Current	[A]
L	Inductance	[H]
P	Power	[W]
R	Resistance	[Ω]
t	Time	[s]
v	Voltage	[V]
θ	Angle	[rad] or [°]
λ	Flux linkage	[Wb]
ω	Rotational speed	[rad/s] or [rpm]
τ	Torque	[Nm]

Acronyms

Abbreviation	Meaning
AC	Alternating Current
FOC	Field Oriented Control
IM	Induction Machine
IPMSM	Interior Permanent Magnet Synchronous Machine
MTPA	Maximum Torque Per Ampere
PMSM	Permanent Magnet Synchronous Machine
PWM	Pulse Width Modulation
SPMSM	Surface Mounted Permanent Magnet Synchronous Machine
VSI	Voltage Source Inverter

Contents

Introduction 1

One of the largest consumers of electric power is the electric machines that convert electric energy into mechanical energy. This caused different energy issues in industrial applications, which led to wide studies to solve the efficiency problems with the purpose of increasing the efficiency of the electric machines. In comparison to the induction machine (IM), the permanent magnet synchronous machine (PMSM), is a popular choice for an AC machine. Because of its higher power density, and higher torque density. During the last decades, it has become important to research the designs and controlling methods for PMSMs in order to improve their torque generation efficiency. Which means the minimization of the overall machine losses. This can be achieved by having a specific design for the machine or by the implementation of complex control techniques. Because the mechanical losses are speed-dependent and can not be controllable, the only losses left that can be minimized are the iron and copper losses. When the machine is operating at lower speeds, the iron losses become negligible compared with the copper losses. This means the optimal operating conditions can be identified as the ones that give minimum copper losses. That would be when the machine is operating with the lowest current magnitude for a given torque, which is called the maximum torque per ampere (MTPA) condition. MTPA control is a common approach to achieve high efficiency and torque density in modern electric machine drive systems. It is easier to achieve the MTPA condition for a Surface Mounted Permanent Magnet Synchronous Machine (SPMSM) when implementing Field-Oriented Control (FOC) because the current vector is normally applied to the machine q-axis. However, for the Interior Permanent Magnet Synchronous Machine (IPMSM), due to the existence of machine saliency, reluctance torque will be introduced and the applied current vector direction to achieve MTPA is no longer aligned with the machine q-axis. Since the machine inductance parameters differ from individual machines and will vary under different operating conditions, it is not implementable to obtain the optimized current vector positions by off-line measurement and calculation. Therefore, on-line MTPA tracking techniques that do not depend on the machine parameters and operation conditions, will be used [1] [2] [3]

1.1 Objectives

The main goal of this project is to investigate, analyze, and realize on-line MTPA tracking technique. The candidate technique will be tested on an SPMSM and an IPMSM platform. The tracking accuracy, reliability, responding speed during transients, and possible influence on the drive system will be examined under different operating conditions.

1.2 Problem Statement

This thesis will answer these main questions:

- *How to implement an on-line MTPA tracking controller for PMSMs?*
- *How to track the accuracy of MTPA controller against system errors and disturbances?*
- *How to test the MTPA convergent speed during system transients, as well as its ability to track varying loads?*

1.3 Assumptions

During the development of this thesis the following assumptions are made:

- In order to get the PMSM to be a balanced three-phase system, the supply voltage is assumed balanced.
- All the losses such as Eddy currents and hysteresis losses are neglected.
- The stator resistance is assumed to be constant and it is not dependent on the changing of the temperature.

System Model 2

2.1 System Description

In order to implement an on-line MTPA tracking controller and investigate the problem statement, a high-performance PMSM drive system is required. The PMSM drive system consists of SPMSM and IPMSM, when the tests in the laboratory are done on the SPMSM, the IPMSM will act as a load system and vice versa. Furthermore, there is a voltage source inverter (VSI), Pulse Width Modulation (PWM), and a dSPACE controller. An overview of the applied drive system is shown in 2.1

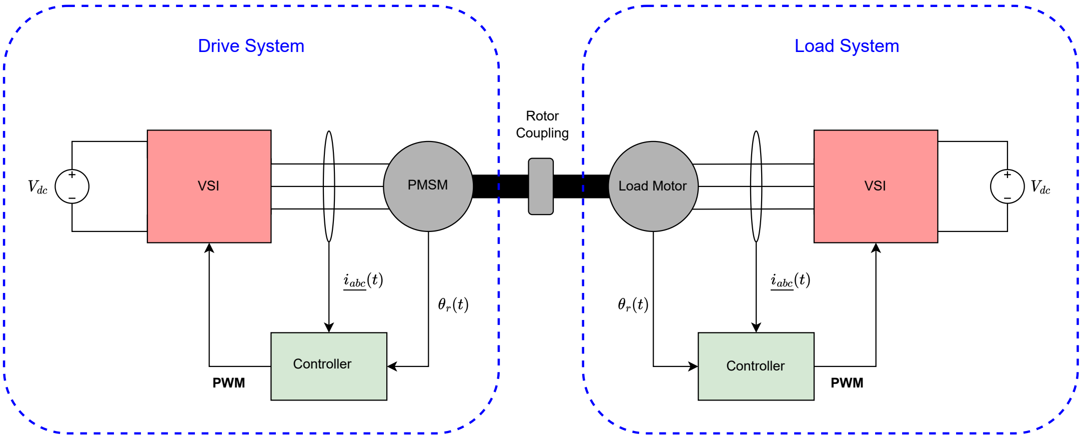

Figure 2.1. An illustration of the test setup: Drive System connected with a Load System

2.2 Modeling of the PMSM

The mathematical model for the PMSM can be described by three equations: voltage, flux linkage, and torque. [4] [5] Using the rotating dq reference frame, the voltage equations are given in 2.1 and 2.2

$$v_d = R_s i_d + \frac{d\lambda_d}{dt} - \omega_e \lambda_q \tag{2.1}$$

$$v_q = R_s i_q + \frac{d\lambda_q}{dt} + \omega_e \lambda_d \tag{2.2}$$

Where v_d, v_q, i_d, i_q are the stator dq-axis voltages and currents respectively. R_s is the single-phase resistance, λ_d and λ_q are the dq-axis flux linkages and ω_e is the electrical rotor speed, which is obtained by multiplying the mechanical rotor speed ω_m by the number of pole pairs p, which can be seen in 2.3

$$\omega_e = p \cdot \omega_m \tag{2.3}$$

The equations for the dq-axis flux linkages are given in 2.4 and 2.5

$$\lambda_d = L_d i_d + \lambda_{mpm} \tag{2.4}$$

$$\lambda_q = L_q i_q \tag{2.5}$$

Where L_d and L_q are the dq-axis inductances and λ_{mpm} is the rotor permanent magnet flux linkage. The equation for the electromagnetic torque is given in 2.6

$$\tau_e = \frac{3}{2} p(\lambda_d i_q - \lambda_q i_d) \tag{2.6}$$

In this project, two types of PMSM have been used, for the SPMSM L_d is approximately equal to L_q, which means the equation for τ_e can be seen in 2.7

$$\tau_e = \frac{3}{2} p \lambda_{mpm} i_q \tag{2.7}$$

However, for the IPMSM L_d is not equal to L_q, and by substituting 2.4 and 2.5 into 2.6 and rearranging, the electromagnetic torque equation for τ_e is given by 2.8

$$\tau_e = \frac{3}{2} p(\lambda_{mpm} i_q + (L_d - L_q) i_d i_q) \tag{2.8}$$

MTPA Control Strategy 3

In this chapter, the MTPA controller will be implemented and investigated for the SPMSM and the IPMSM drive system. [1] [2] [3]

3.1 MTPA Point Characterization and Operation Point

The MTPA control strategy can be described as an optimization problem with the aim of minimizing the current for a given torque reference. By using the torque equation 2.7 for PMSM, the set parameter can only be i_q because L_d is equal to L_q. However, for IPMSM L_d is not equal to L_q and the torque equation is 3.1 for the IPMSM, which can be rewritten as 3.2 and the set parameters can either be the i_q and i_d currents or the magnitude of the current vector i_s or the angle φ

$$\tau_e = \frac{3}{2}p(\lambda_{mpm}i_q + (L_d - L_q)i_d i_q) \tag{3.1}$$

$$\tau_e = \frac{3}{2}p(\lambda_{mpm}i_s \sin(\varphi) + \frac{3}{2}p(L_d - L_q){i_s}^2 \sin(\varphi)) \tag{3.2}$$

The MTPA operating condition can only be achieved for the combination that yields the minimum current magnitude $\mid i(i_d, i_q) \mid = \sqrt{{i_d}^2 + {i_q}^2}$ which means the combination that solves the following constrained optimization problem:

min $\mid i(i_d, i_q) \mid$ subject to $\tau(i_d, i_q) = \tau_0$

In the case of PMSM the above minimization problem can be solved by having $i_d = 0$. However, for IPMSM it can be seen in the graphical representation of the MTPA operating points in figure 3.1

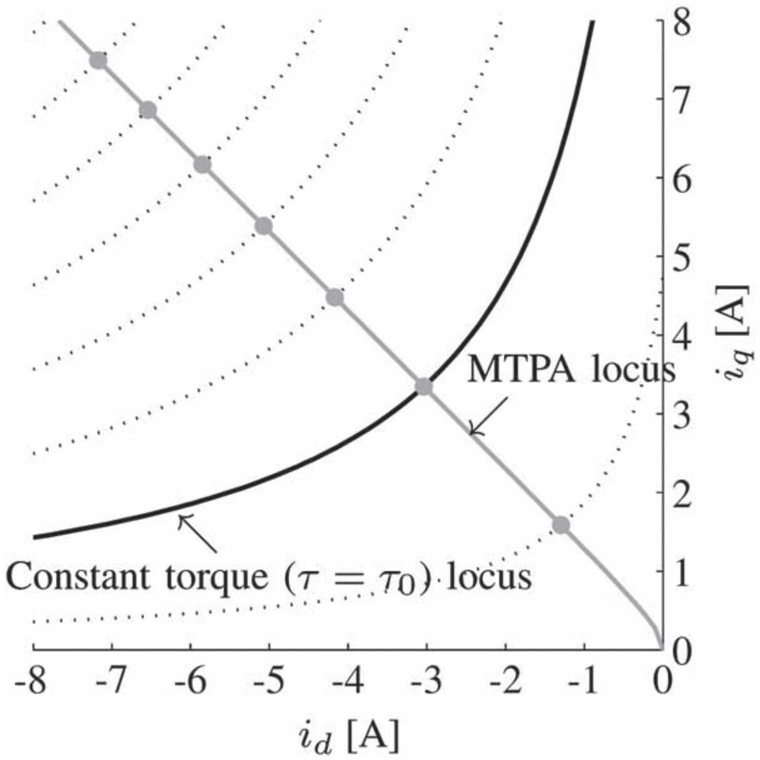

Figure 3.1. A graphical representation of the MTPA operating points for an IPMSM

However, using this method in order to find the MTPA operating point is inaccurate because the equations represent a linearised ideal model of the machine. In reality, the machine parameters change due to temperatures, and there would be disturbance due to load changes.

3.1.1 Finding MTPA Operating Points and Curves

In this project, some tests have been done in the lab in order to find the MTPA operating point for SPMS and IPMSM as well as the MTPA oerating curves, which later on will be used to verify the MTPA Strategy.

For SPMSM:

The MTPA operating points

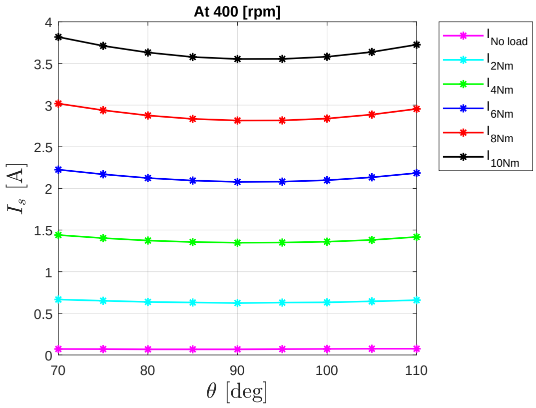

Figure 3.2. MTPA operating points for SPMSM at 400 rpm

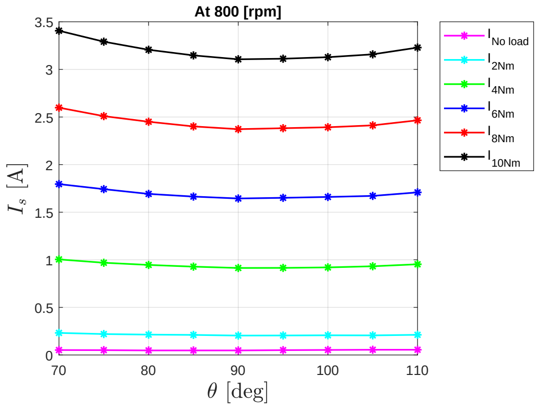

Figure 3.3. MTPA operating points for SPMSM at 800 rpm

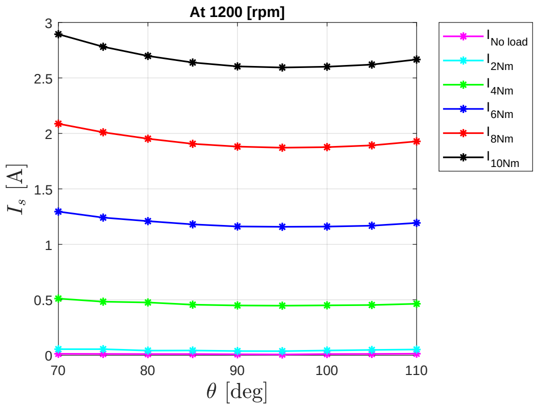

Figure 3.4. MTPA operating points for SPMSM at 1200 rpm

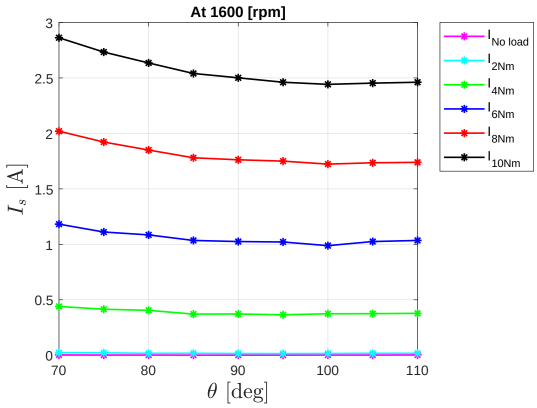

Figure 3.5. MTPA operating points for SPMSM at 1600 rpm

The MTPA operating curves

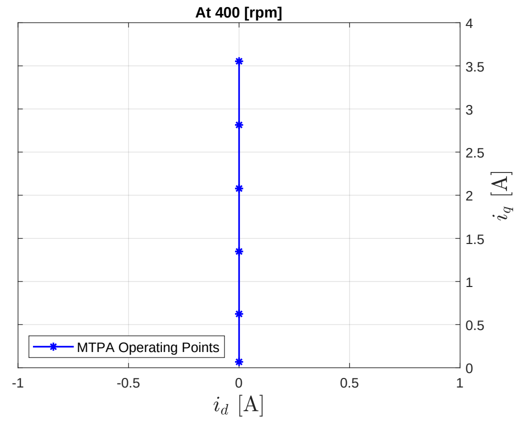

Figure 3.6. MTPA operating curve for SPMSM at 400 rpm

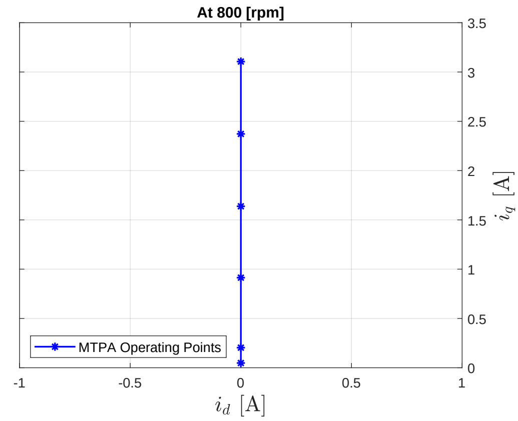

Figure 3.7. MTPA operating curve for SPMSM at 800 rpm

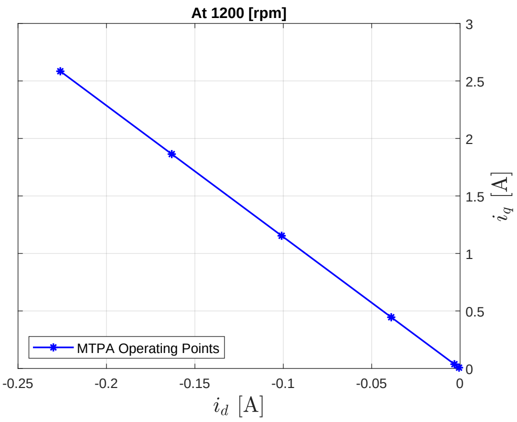

Figure 3.8. MTPA operating curve for SPMSM at 1200 rpm

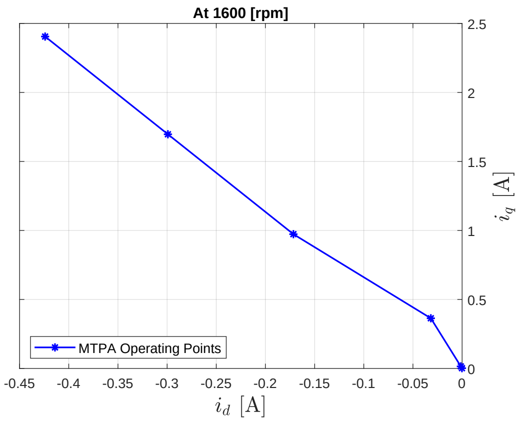

Figure 3.9. MTPA operating curve for SPMSM at 1600 rpm

For IPMSM

The MTPA operating points

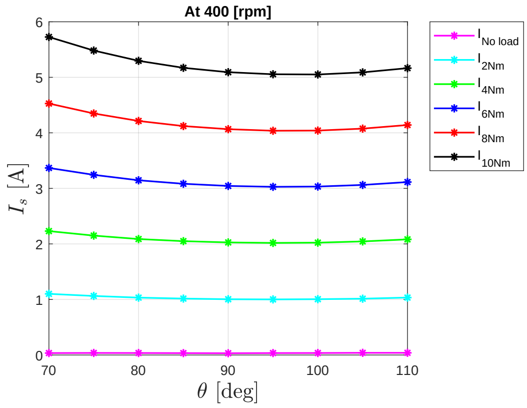

Figure 3.10. MTPA operating points for IPMSM at 400 rpm

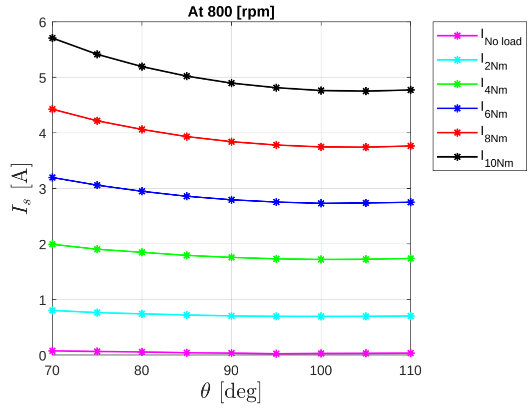

Figure 3.11. MTPA operating points for IPMSM at 800 rpm

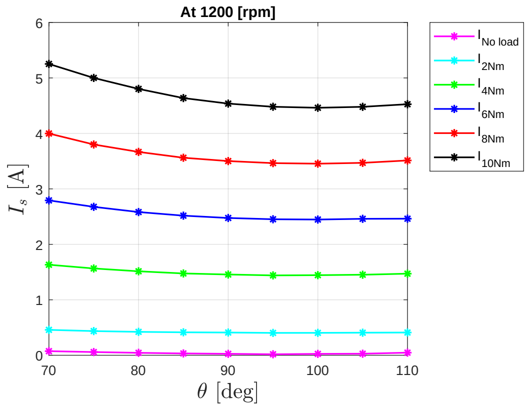

Figure 3.12. MTPA operating points for IPMSM at 1200 rpm

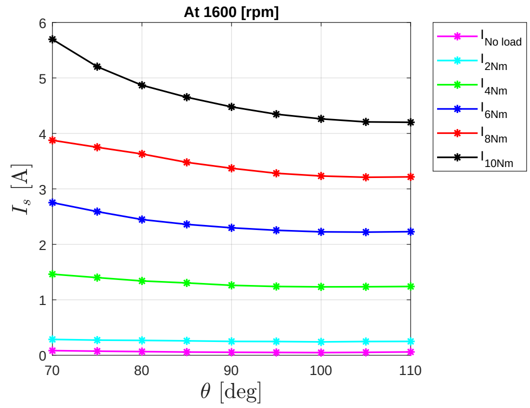

Figure 3.13. MTPA operating points for IPMSM at 1600 rpm

The MTPA operating curves

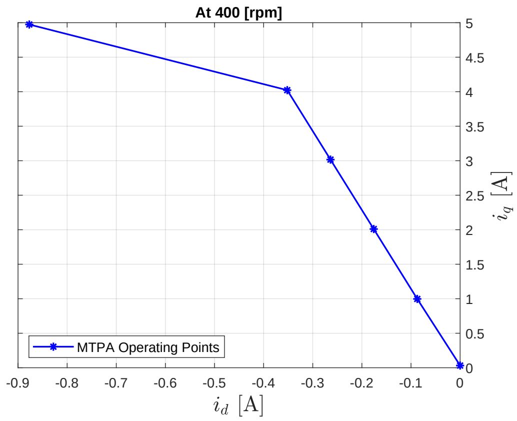

Figure 3.14. MTPA operating curve for IPMSM at 400 rpm

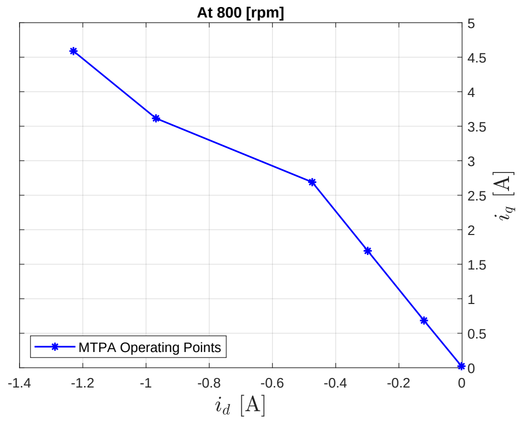

Figure 3.15. MTPA operating curve for IPMSM at 800 rpm

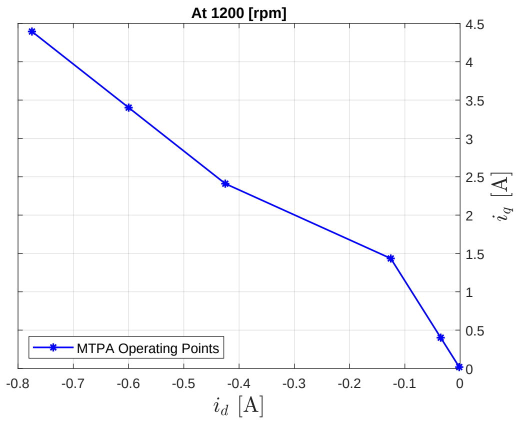

Figure 3.16. MTPA operating curve for IPMSM at 1200 rpm

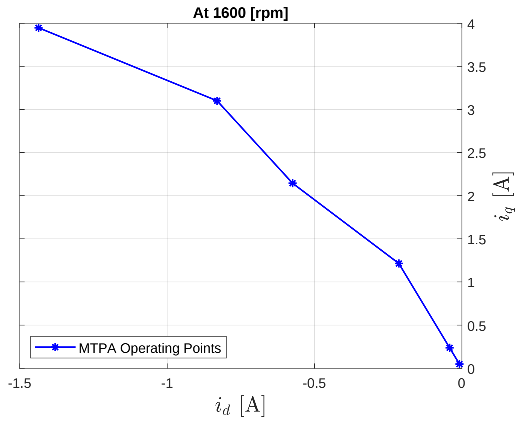

Figure 3.17. MTPA operating curve for IPMSM at 1600 rpm

3.2 MTPA Control Strategy

This MTPA control strategy uses a signal injection tracking technique to perturb the current angle and determine the changing rate of the current magnitude with respect to the current angle until a global minimum for the cost function is reached $di/d\varphi = 0$ which can be seen in figure 3.18

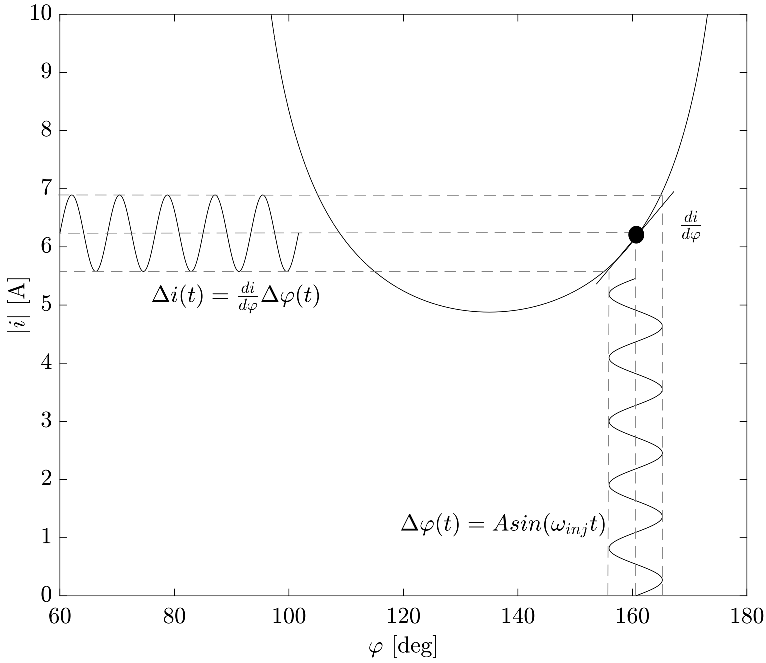

Figure 3.18. Graphical representation of the MTPA operating points for an IPMSM based on signal injection method to determine the slope of the cost function

Which means this method will increase the phase of the current φ whenever the slope is negative and decrease it when the slope is positive. The equation for the injected signal that is applied to the current is

$$\Delta\varphi(t) = A\sin(\omega_{inj}t) \tag{3.3}$$

A block diagram for the MTPA controller can be seen in figure 3.19

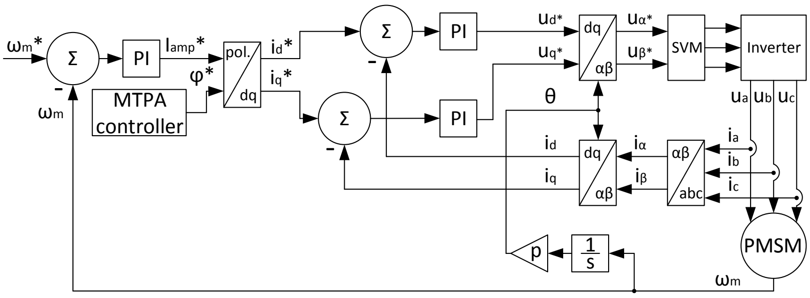

Figure 3.19. Block diagram for the MTPA controller

The gain factors for this MTPA tracking technique were found experimentally in the lab for the SPMSM and IPMSM, which can be seen in figure 3.20 and figure **??**

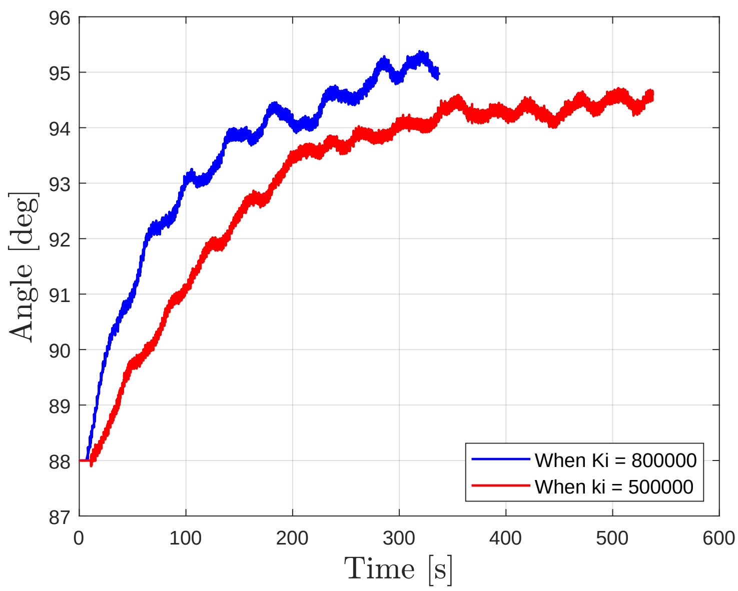

Figure 3.20. Gain factor for MTPA for IPMSM

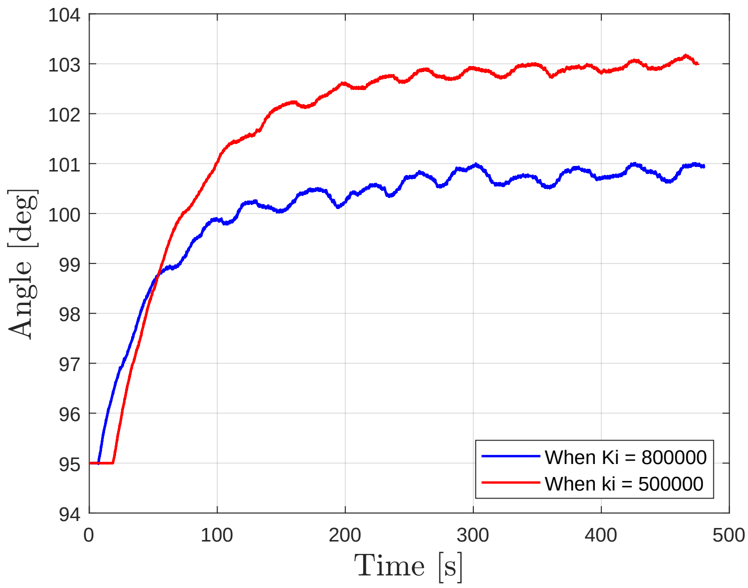

Figure 3.21. Affects of the gain factor for MTPA for IPMSM

Two different types of filters were implemented in this MTPA control strategy in order to achieve better results. The first one is a low-pass filter and the second one is a resonant filter. A comparison of their effects can be seen in Figure 3.22 and 3.23

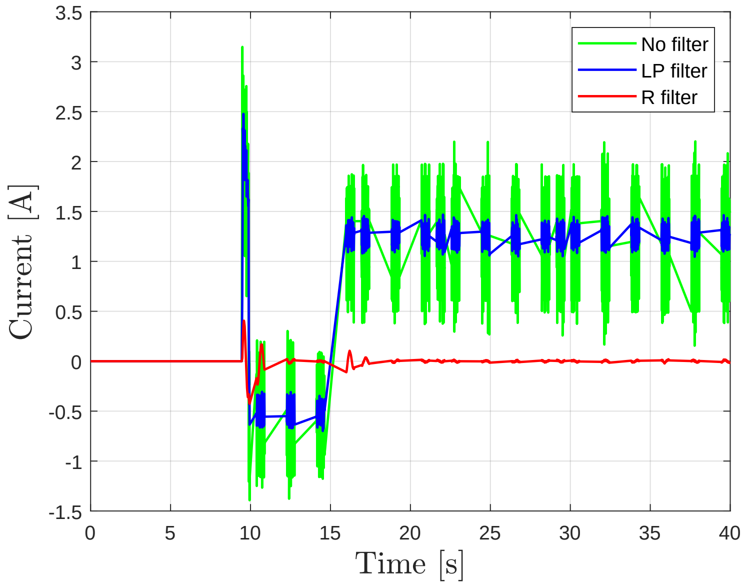

Figure 3.22. Affects of the two filters on the MTPA controller for SPMSM

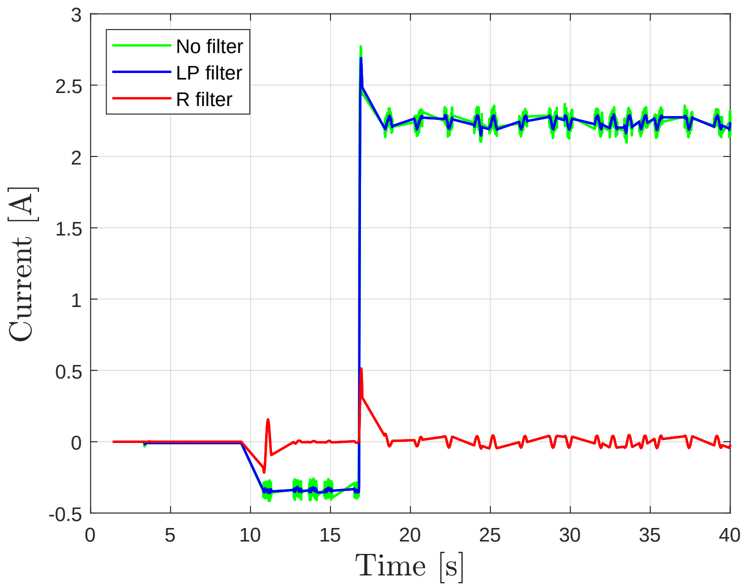

Figure 3.23. Affects of the two filters on the MTPA controller for SPMSM

The equations for the low-pass filter is 3.4

$$H_{LPF} = \frac{\omega_c}{s + \omega_c} \tag{3.4}$$

Where ω_c is equal to $2\pi f_c$ f_c is the switching frequency

The equation for the resonant filter is 3.5 [6]

$$G_s = \frac{2K_i\omega_c s}{s^2 + 2\omega_c + \omega^2} \tag{3.5}$$

Experimental Results 4

4.1 MTPA Results for SPMSM

4.1.1 Steady State at 400 [rpm]

For a starting current angle at 80°

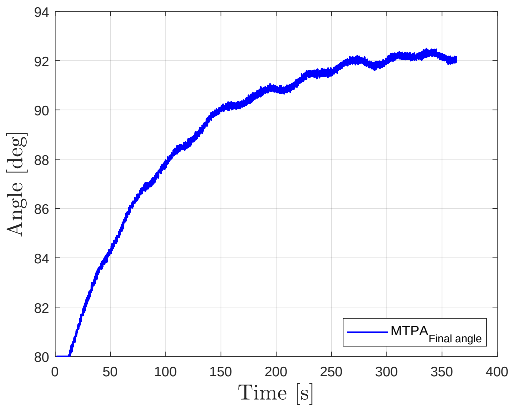

Figure 4.1. Final current angle at 400 rpm and 2 Nm load torque

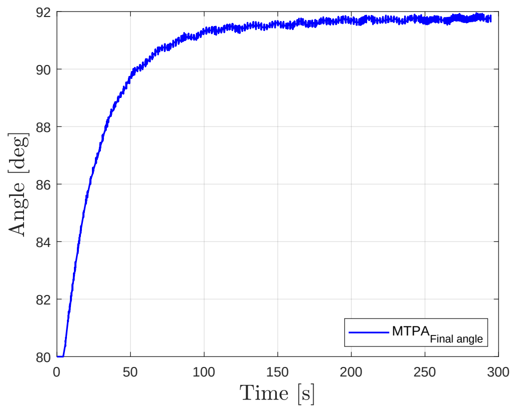

Figure 4.2. Final current angle at 400 rpm and 6 Nm load torque

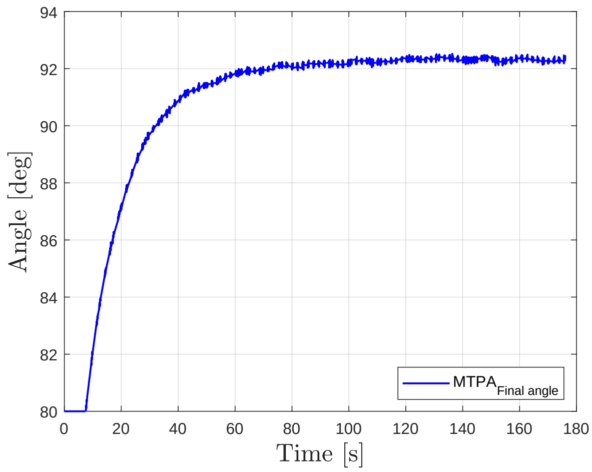

Figure 4.3. Final current angle at 400 rpm and 10 Nm load torque

For a starting current angle at $100°$

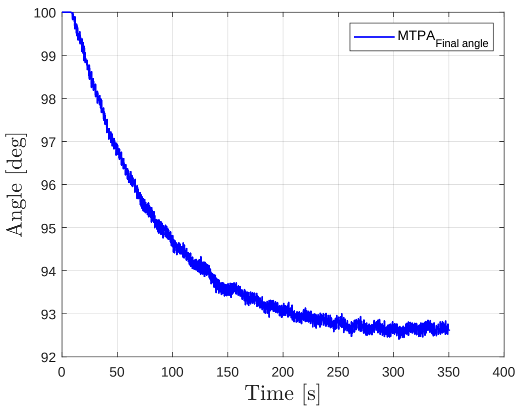

Figure 4.4. Final current angle at 400 rpm and 2 Nm load torque

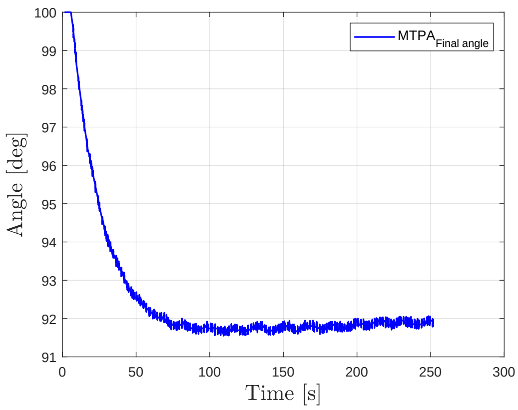

Figure 4.5. Final current angle at 400 rpm and 6 Nm load torque

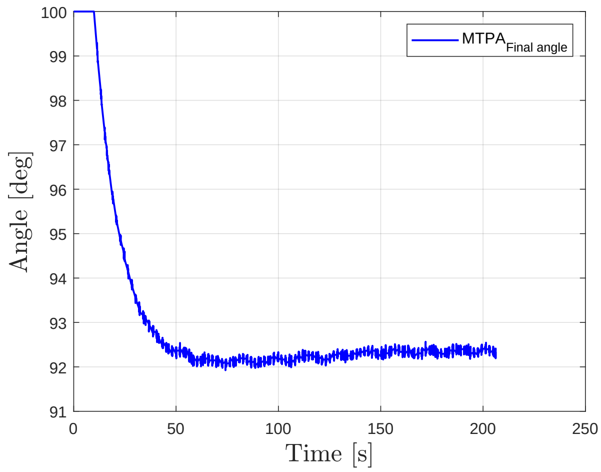

Figure 4.6. Final current angle at 400 rpm and 10 Nm load torque

4.1.2 Steady State at 800 [rpm]

For a starting current angle at 80°

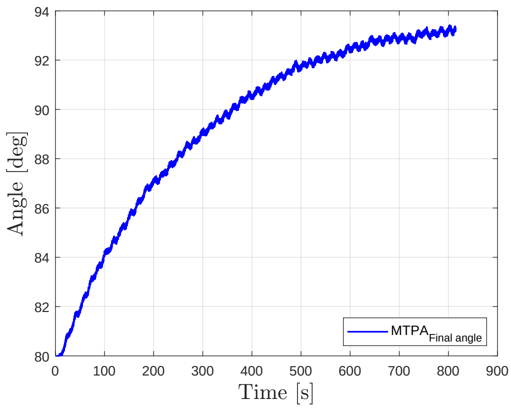

Figure 4.7. Final current angle at 800 rpm and 2 Nm load torque

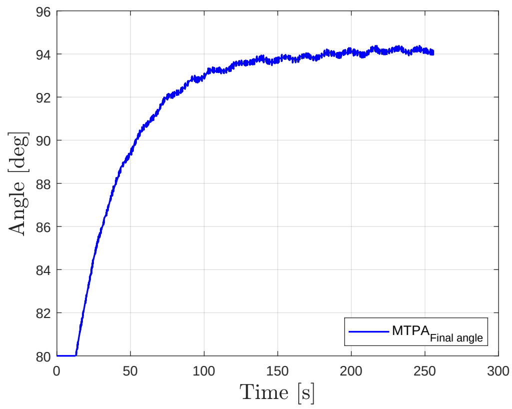

Figure 4.8. Final current angle at 800 rpm and 6 Nm load torque

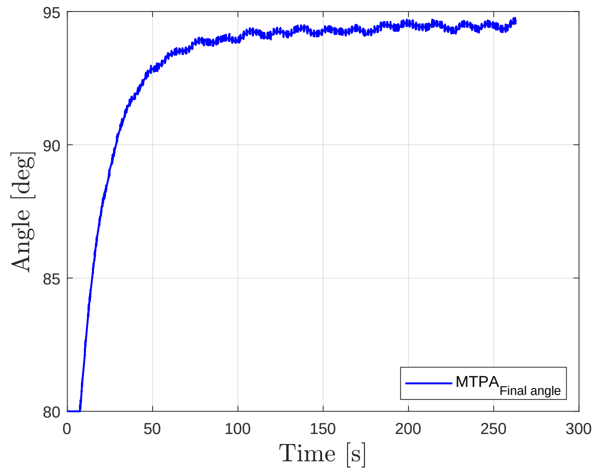

Figure 4.9. Final current angle at 800 rpm and 10 Nm load torque

For a starting current angle at 100°

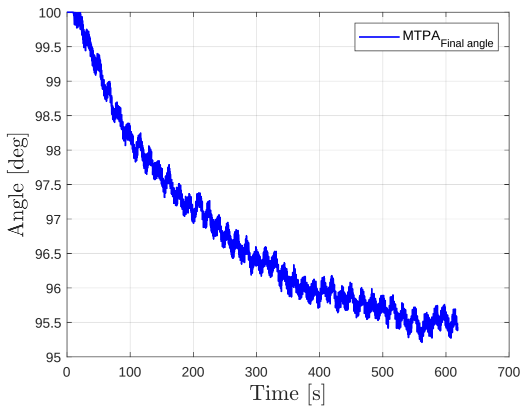

Figure 4.10. Final current angle at 800 rpm and 2 Nm load torque

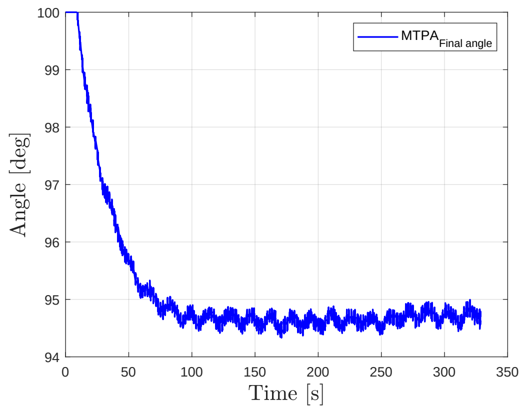

Figure 4.11. Final current angle at 800 rpm and 6 Nm load torque

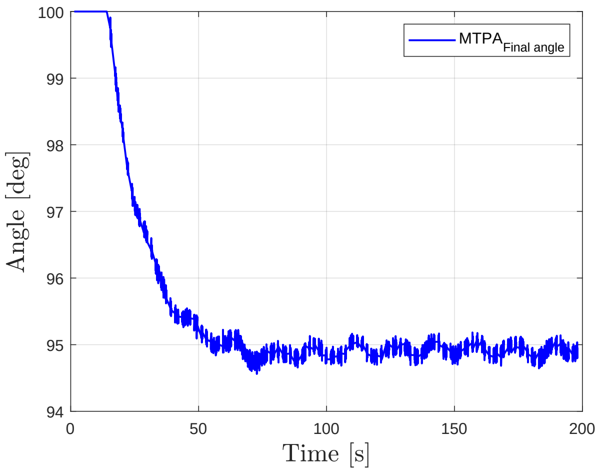

Figure 4.12. Final current angle at 800 rpm and 10 Nm load torque

4.1.3 Steady State at 1200 [rpm]

For a starting current angle at 80°

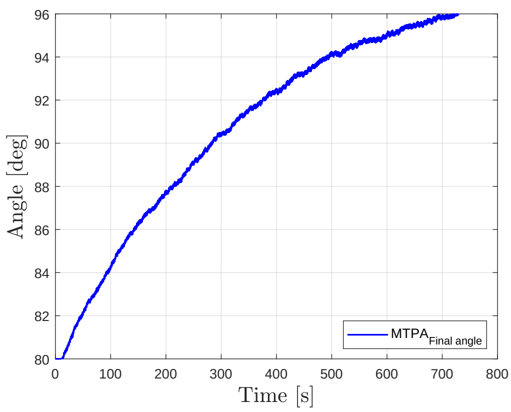

Figure 4.13. Final current angle at 1200 rpm and 2 Nm load torque

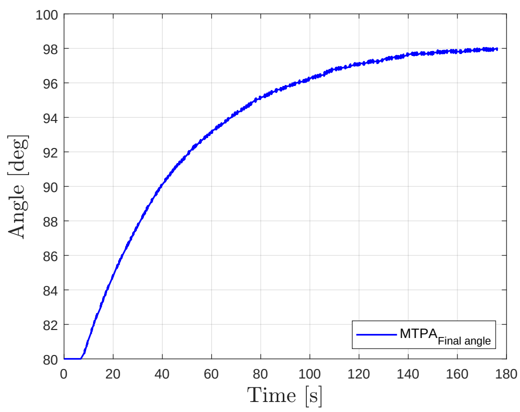

Figure 4.14. Final current angle at 1200 rpm and 6 Nm load torque

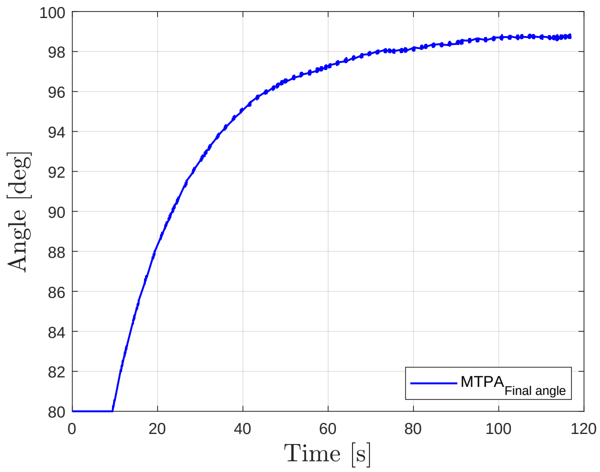

Figure 4.15. Final current angle at 1200 rpm and 10 Nm load torque

For a starting current angle at $100°$

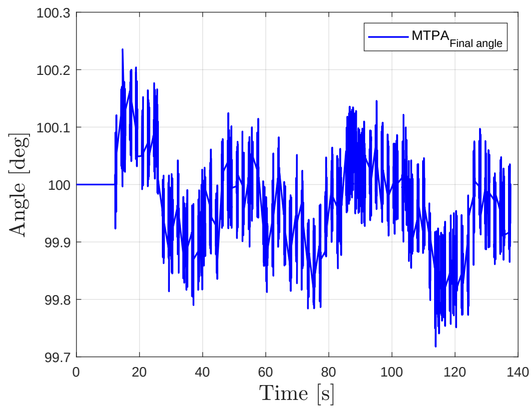

Figure 4.16. Final current angle at 1200 rpm and 2 Nm load torque

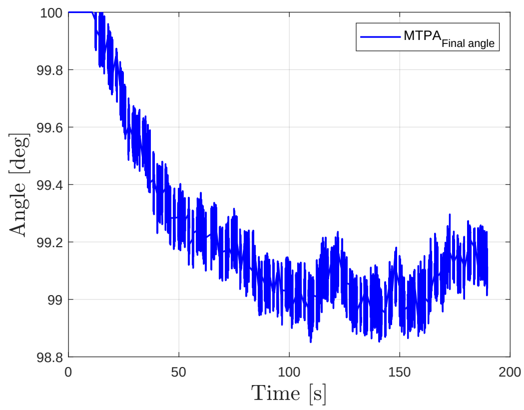

Figure 4.17. Final current angle at 1200 rpm and 6 Nm load torque

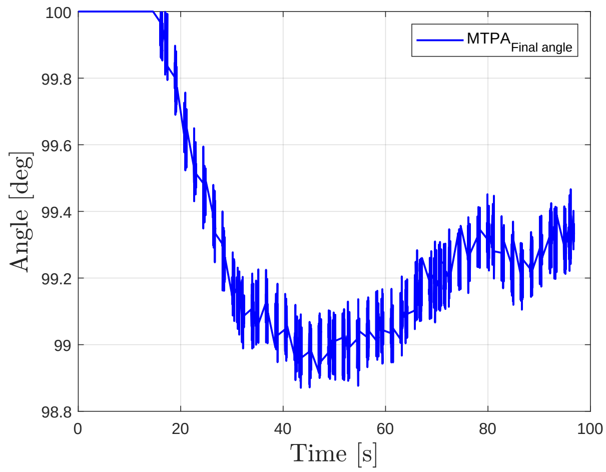

Figure 4.18. Final current angle at 1200 rpm and 10 Nm load torque

4.1.4 Steady State at 1600 [rpm]

For a starting current angle at 80°

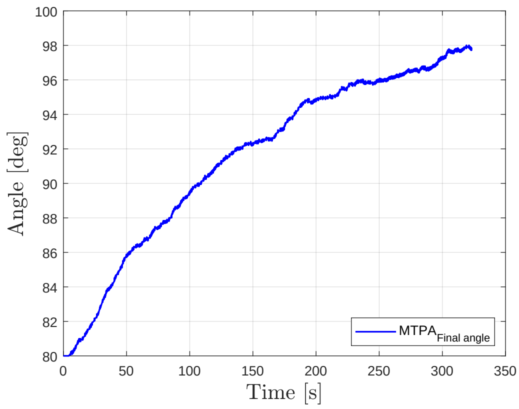

Figure 4.19. Final current angle at 1600 rpm and 2 Nm load torque

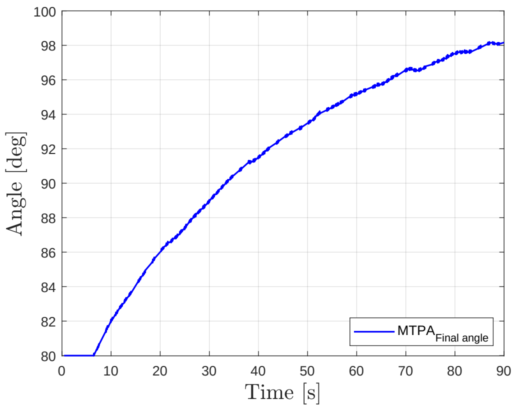

Figure 4.20. Final current angle at 1600 rpm and 6 Nm load torque

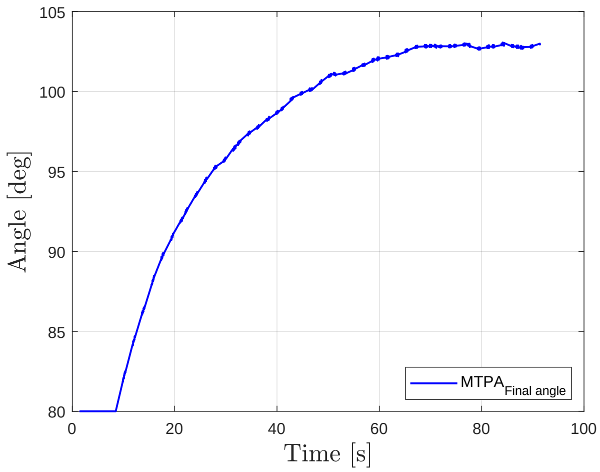

Figure 4.21. Final current angle at 1600 rpm and 10 Nm load torque

For a starting current angle at 100°

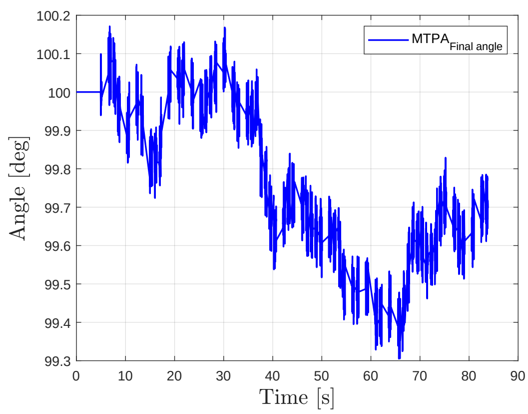

Figure 4.22. Final current angle at 1600 rpm and 2 Nm load torque

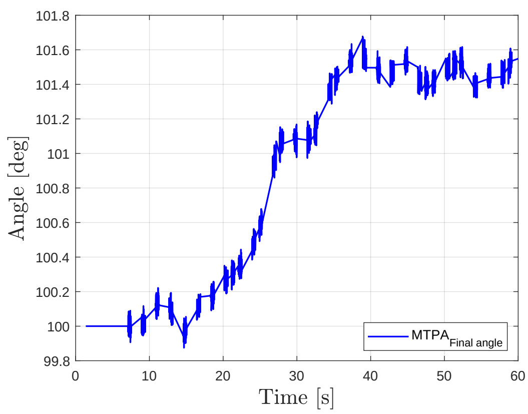

Figure 4.23. Final current angle at 1600 rpm and 6 Nm load torque

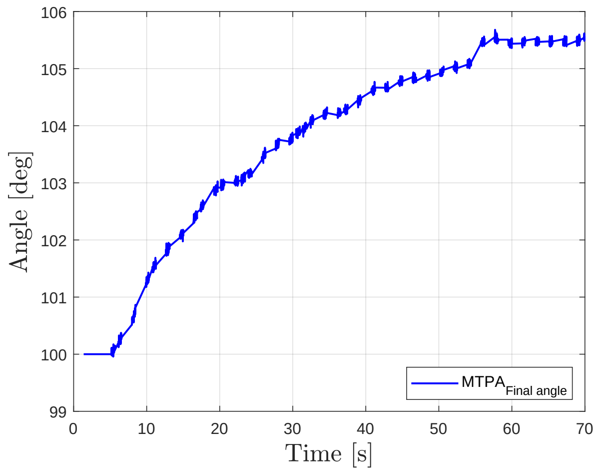

Figure 4.24. Final current angle at 1600 rpm and 10 Nm load torque

4.1.5 Step Changes Tests

Speed Step Change

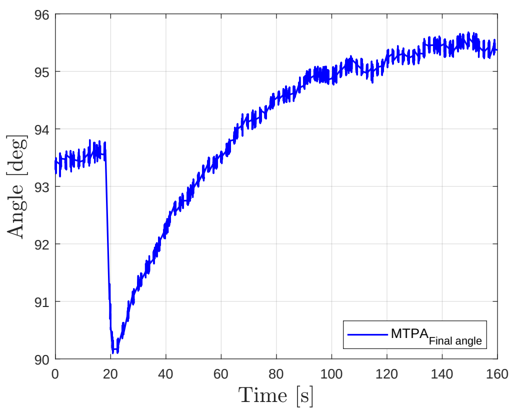

Figure 4.25. Final current angle at speed step change from 400 rpm to 800 rpm

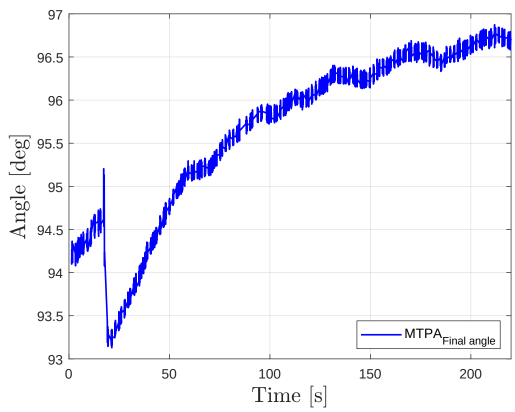

Figure 4.26. Final current angle at speed step change from 800 rpm to 1200 rpm

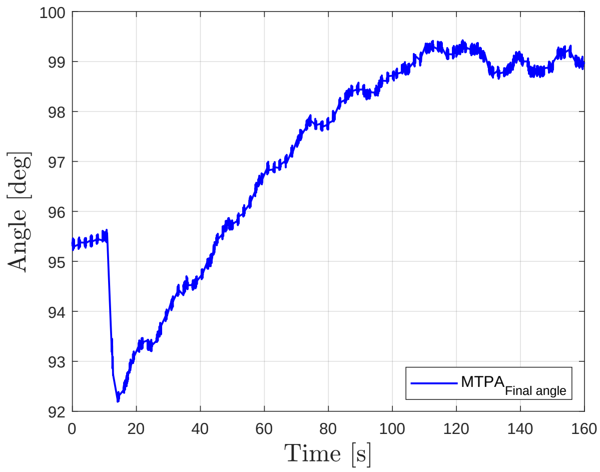

Figure 4.27. Final current angle at speed step change from 1200 rpm to 1600 rpm

Load Step Change

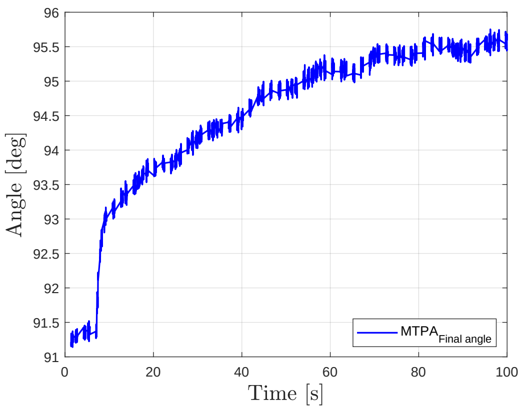

Figure 4.28. Final current angle at load step change from 2 Nm to 6 Nm

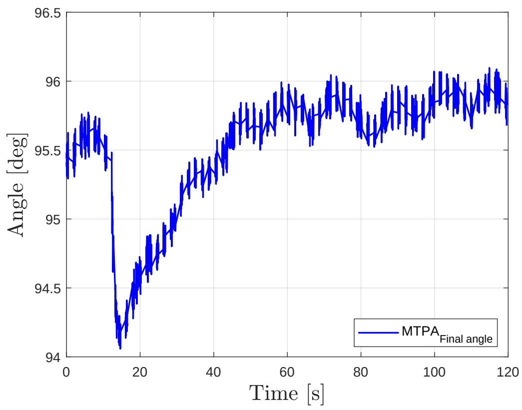

Figure 4.29. Final current angle at load step change from 6 Nm to 10 Nm

4.2 MTPA Results for IPMSM

4.2.1 Steady State at 400 [rpm]

For a starting current angle at 80°

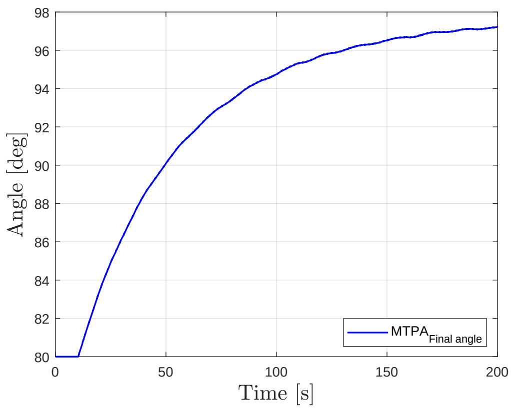

Figure 4.30. Final current angle at 400 rpm and 2 Nm load torque

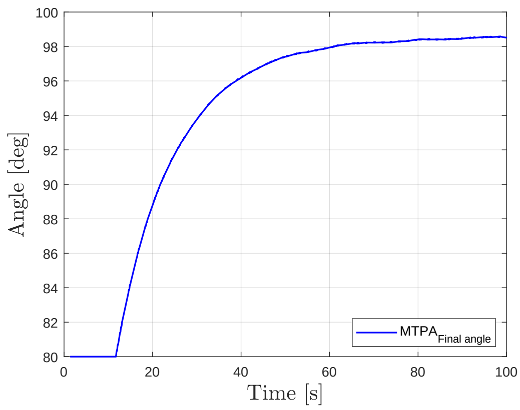

Figure 4.31. Final current angle at 400 rpm and 6 Nm load torque

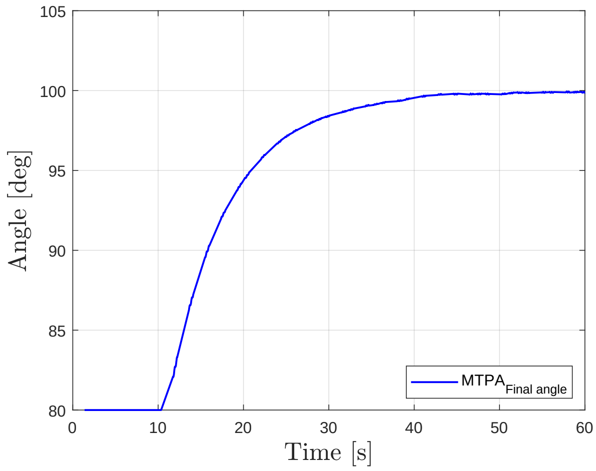

Figure 4.32. Final current angle at 400 rpm and 10 Nm load torque

For a starting current angle at 100°

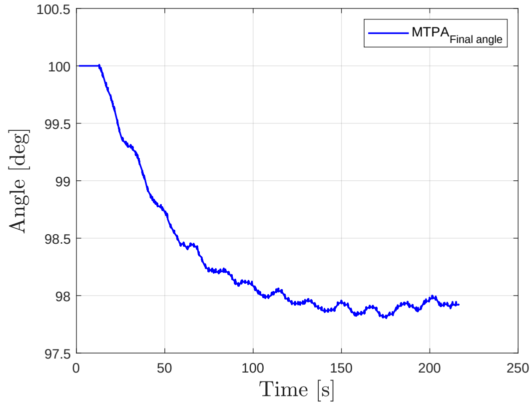

Figure 4.33. Final current angle at 400 rpm and 2 Nm load torque

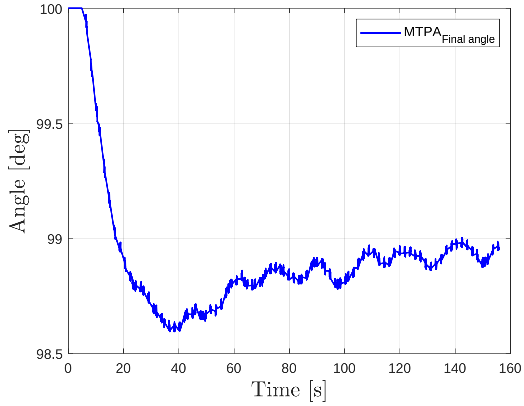

Figure 4.34. Final current angle at 400 rpm and 6 Nm load torque

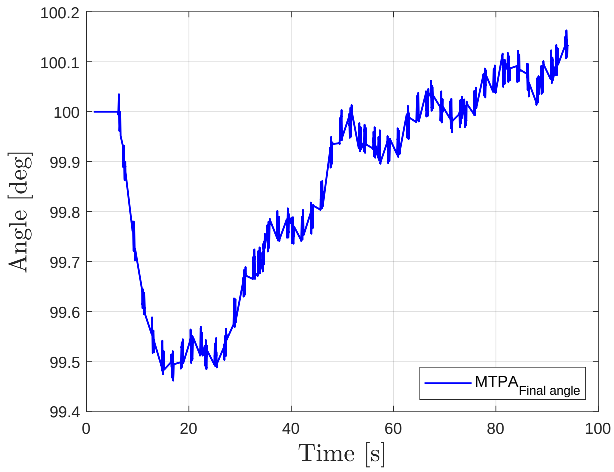

Figure 4.35. Final current angle at 400 rpm and 10 Nm load torque

4.2.2 Steady State at 800 [rpm]

For a starting current angle at 80°

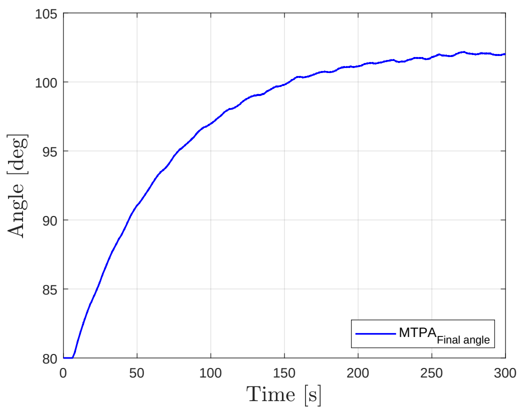

Figure 4.36. Final current angle at 800 rpm and 2 Nm load torque

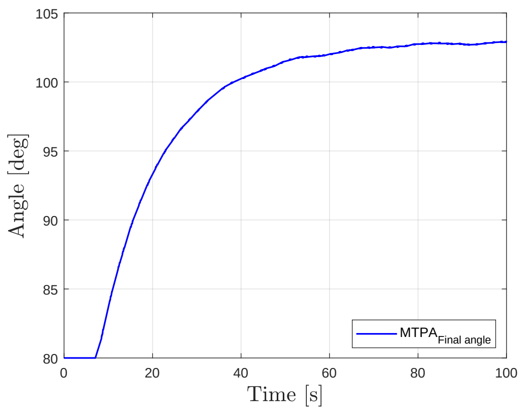

Figure 4.37. Final current angle at 800 rpm and 6 Nm load torque

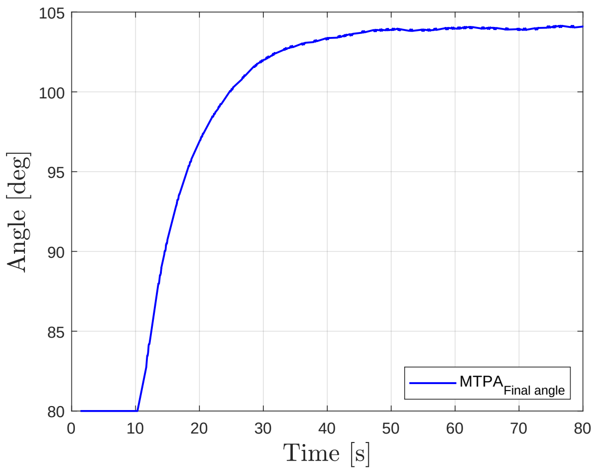

Figure 4.38. Final current angle at 800 rpm and 10 Nm load torque

For a starting current angle at 100°

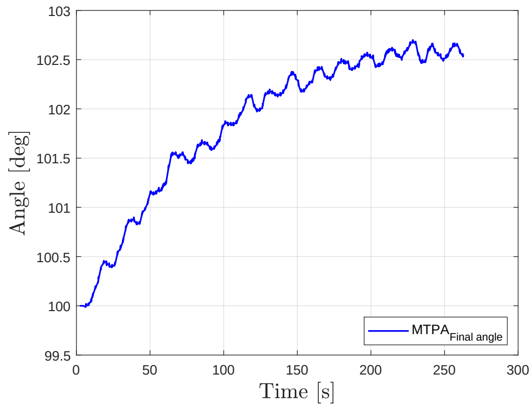

Figure 4.39. Final current angle at 800 rpm and 2 Nm load torque

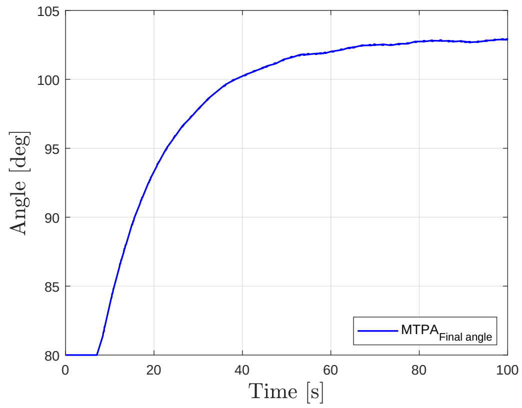

Figure 4.40. Final current angle at 800 rpm and 6 Nm load torque

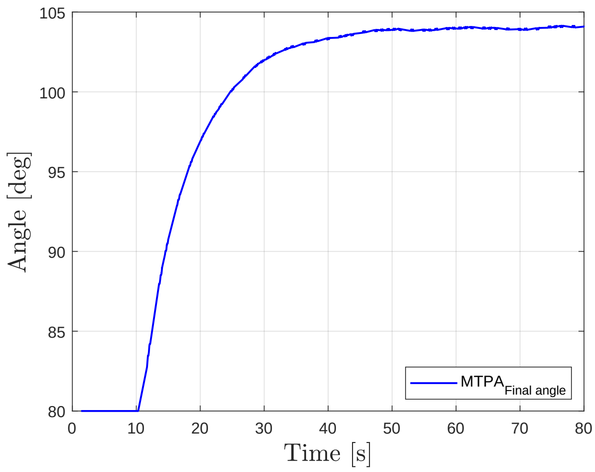

Figure 4.41. Final current angle at 800 rpm and 10 Nm load torque

4.2.3 Steady State at 1200 [rpm]

For a starting current angle at 80°

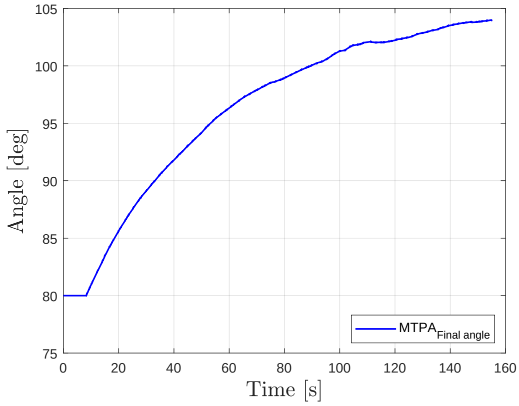

Figure 4.42. Final current angle at 1200 rpm and 2 Nm load torque

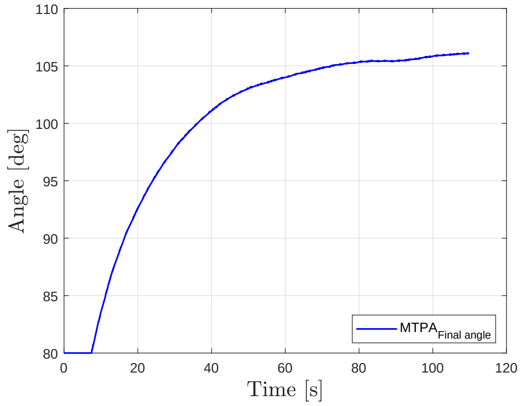

Figure 4.43. Final current angle at 1200 rpm and 6 Nm load torque

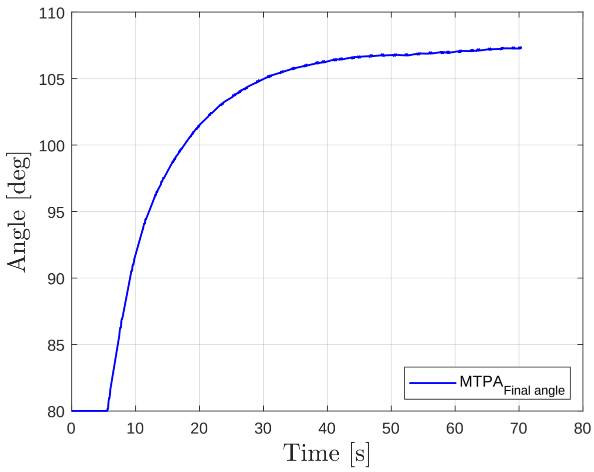

Figure 4.44. Final current angle at 1200 rpm and 10 Nm load torque

For a starting current angle at $100°$

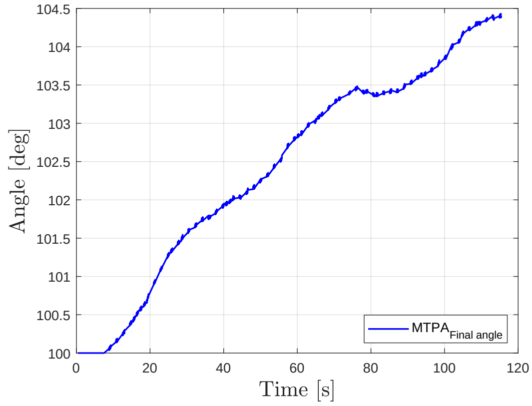

Figure 4.45. Final current angle at 1200 rpm and 2 Nm load torque

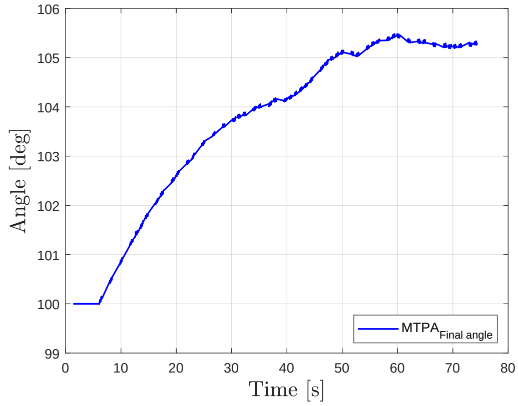

Figure 4.46. Final current angle at 1200 rpm and 6 Nm load torque

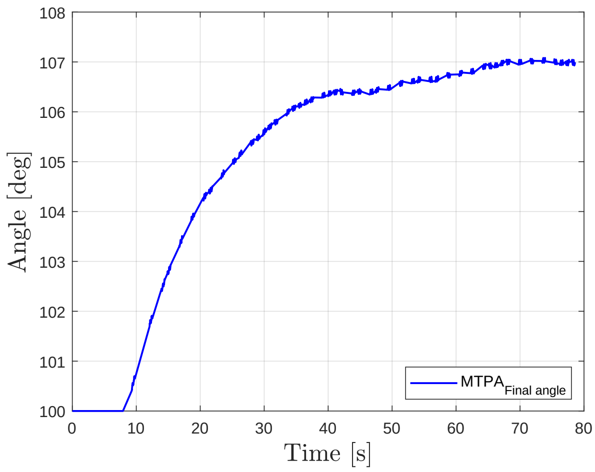

Figure 4.47. Final current angle at 1200 rpm and 10 Nm load torque

4.2.4 Step Changes Tests

Speed Step Change

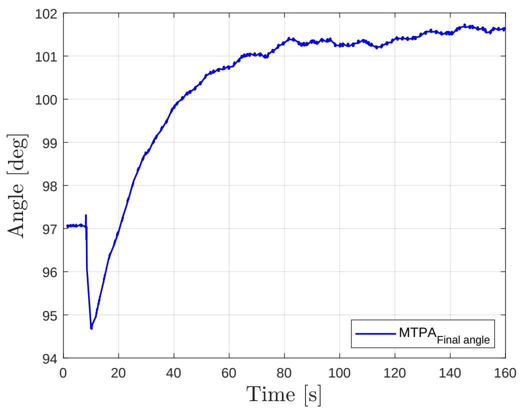

Figure 4.48. Final current angle at speed step change from 400 rpm to 800 rpm

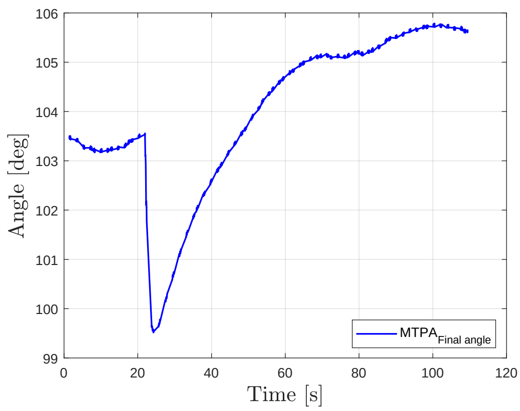

Figure 4.49. Final current angle at speed step change from 800 rpm to 1200 rpm

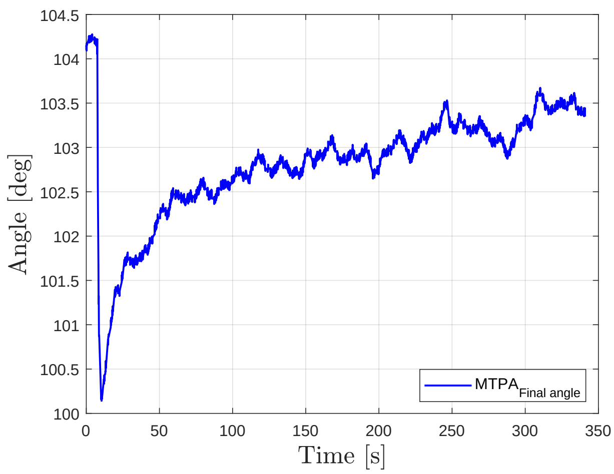

Figure 4.50. Final current angle at speed step change from 1200 rpm to 1600 rpm

Load Step Change

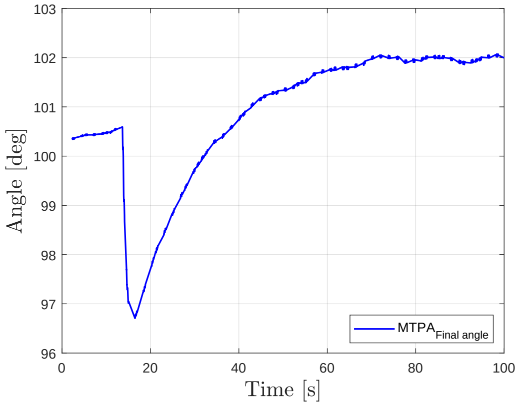

Figure 4.51. Final current angle at load step change from 2 Nm to 6 Nm

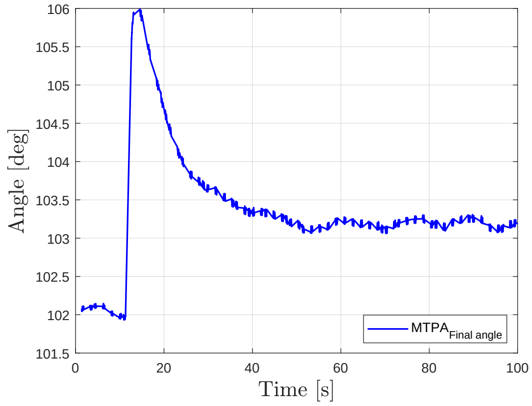

Figure 4.52. Final current angle at load step change from 6 Nm to 10 Nm

Discussion and Conclusion 5

5.1 For SPMSM

After comparing the results of the final current angles at different speeds with the MTPA points and curves that have been found in 3.1.1, it is possible to say the MTPA control strategy works for SPMSM. Furthermore, the MTPA also works for the speed and load step changes.

5.2 For IPMSM

After comparing the results of the final current angles at different speeds with the MTPA points and curves that have been found in 3.1.1, it is possible to say that the MTPA control strategy works for IPMSM. Furthermore, the MTPA also works for the speed and load step changes.

Bibliography

[1] Riccardo Antonello, Matteo Carraro, and Mauro Zigliotto. Maximum-torque-per-ampere operation of anisotropic synchronous permanent-magnet motors based on extremum seeking control. *IEEE Transactions on Industrial Electronics*, 61(9):5086–5093, Sept 2014.

[2] Sungmin Kim, Young-Doo Yoon, Seung-Ki Sul, and Kozo Ide. Maximum torque per ampere (mtpa) control of an ipm machine based on signal injection considering inductance saturation. *IEEE Transactions on Power Electronics*, 28(1):488–497, Jan 2013.

[3] Silverio Bolognani, Luca Peretti Yoon, and Mauro Zigliotto. Online mtpa control strategy for dtc synchronous-reluctance-motor drives. *IEEE Transactions on Power Electronics*, 26(1):20–28, Jan 2011.

[4] Ned Mohan, Tore M. Undeland, and William P. Robbins. *Power Electronics, 3th edition.* Number ISBN: 978-0-471-22693-2 in Paperback. John Wiley and Sons, Inc., 2003.

[5] Charles L. Phillips and John M. Parr. *Feedback Control System, 5th edition.* Number ISBN: 978-0-13-186614-0 in Paperback. 2000 Pearson Education, Inc., 2011.

[6] Dong Wang, Kaiyuan Lu Yoon, and Peter Omand Rasmussen. Improved closed-loop flux observer based sensorless control against system oscillation for synchronous reluctance machine drives. *IEEE Transactions on Power Electronics*, 34(5):4593–4602, May 2019.